International Journal of Mechanical, Industrial and Aerospace Sciences
ISSN: 2517-9950
Vol:7, No:12, 2013

Behaviours of Energy Spectrum at Low Reynolds Numbers in Grid Turbulence

Md. Kamruzzaman, L. Djenidi, R. A. Antonia

***Abstract*—**This paper reports an experimental investigation of the energy spectrum of turbulent velocity fields at low Reynolds numbers (R_λ) in grid turbulence. Hot wire measurements are carried out in grid turbulence with subjected to a 1.36:1 contraction of the wind tunnel. Three different grids are used: (i) large square perforated grid (mesh size 43.75 mm), (ii) small square perforated grid (mesh size 14. and (iii) woven mesh grid (mesh size 5mm). The results indicate that the energy spectrum at small R_λ does not follow Kolmogorov's universal scaling. It is further found that the critical Reynolds number, $R_{\lambda,c}$ below which the scaling breaks down, is around 25.

***Keywords*—**Decay exponent, Energy spectrum, Taylor microscale Reynolds number, Taylor microscale, Turbulent kinetic energy.

I. Introduction

GRID turbulence is an important fundamental turbulent flow because it represents a close approximation of homogeneous isotropic turbulence (hereafter, HIT). The turbulence is generated by inserting a grid (for example: a perforated plate or a woven mesh grid) in a uniform flow. The turbulence decays because there is no turbulent production.

Kolmogorov's first similarity hypothesis describes that the spectra of velocity fluctuations scale on the kinematic viscosity (ν) and the turbulent kinetic energy dissipation rate $\langle\varepsilon\rangle$ at sufficiently large Reynolds numbers R_λ based on the Taylor microscale [1]. Experimental and numerical evidence demonstrate that the scaling also holds moderately low R_λ (e.g. [2], [3]). This aspect was recently exploited by [4] to develop a spectral chart method for correct estimating $\langle\varepsilon\rangle$ various different turbulent flows. However, one can wonder if the Kolmogorov scaling still holds when R_λ reaches relatively small values for the energy transfer to become small. The present work is aimed at investigating whether the Kolmogorov scaling holds or not at low Reynolds number, and if so to estimate the critical value of R_λ below which the Kolmogorov scaling breaks down.

The present work complements and extends that of numerical studies of [5] and [6]. These authors found that the Kolmogorov scaling breaks down when R_λ falls down below about 20.

Md. Kamruzzaman, PhD student, Discipline of Mechanical Engineering, The University of Newcastle, Callaghan 2308, NSW, Australia (corresponding author to provide phone: +61-0432681792; e-mail: c3160016@uon.edu.au).

Djenidi, L. is a professor, Discipline of Mechanical Engineering, The University of Newcastle, Callaghan 2308, NSW, Australia (e-mail: lyazid.djenidi@newcastle.edu.au).

R.A. Antonia is an emeritus professor, Department of Mechanical Engineering, University of Newcastle, Callaghan 2308, NSW, Australia (e-mail: Robert.Antonia@ newcastle.edu.au).

II. Experimental Apparatus

Three grids are used: two perforated and a woven mesh. Fig. 1 shows two perforated plates. The first (Lsq43) plate consists of large square holes (mesh $M = 43.75mm$) and the second (Ssq43) of small square holes (mesh $M = 14.15$ mm). The solidity (defined as $\sigma = d/M(2-d/M)$) of the two grids is $\sigma = 43\%$. The mesh ratio of Lsq43 to Ssq43 is 3:1 approximately. The third grid consists of interwoven vertical and horizontal bard with solidity $\sigma = 36\%$.

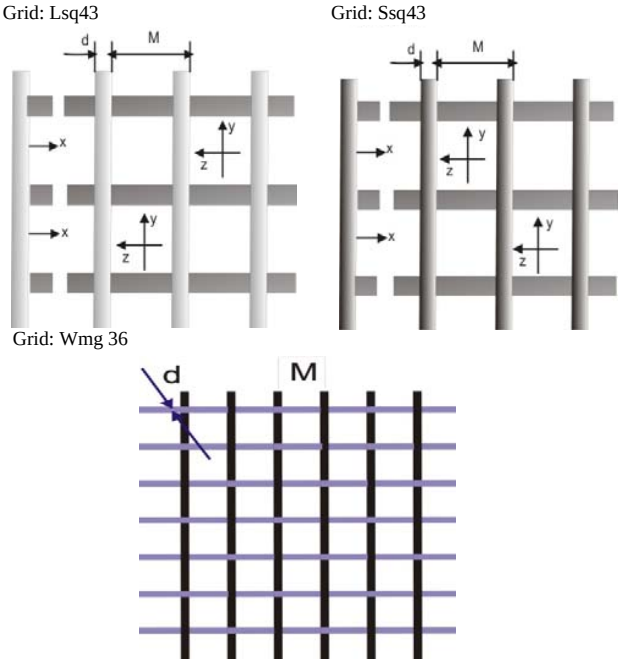

Fig. 1 The geometry of two different perforated grids and one woven mesh grid; *x* coordinates axis lies on the centreline of the flow

Fig. 2 shows a schematic diagram of the open circuit wind tunnel that [7] and [8] previously used. The air flow is driven by a centrifugal blower which is controlled by a variable-cycle (0-1,500 rpm) power supply. To minimize vibration, the blower is supported by dampers and is connected to the tunnel by a flexible joint. At the inlet to the platinum, an air filter

(594 mm × 594 mm × 96 mm long) captures particles from the flow and a honeycomb ($l/d \approx 4.3$) removes residual swirl.

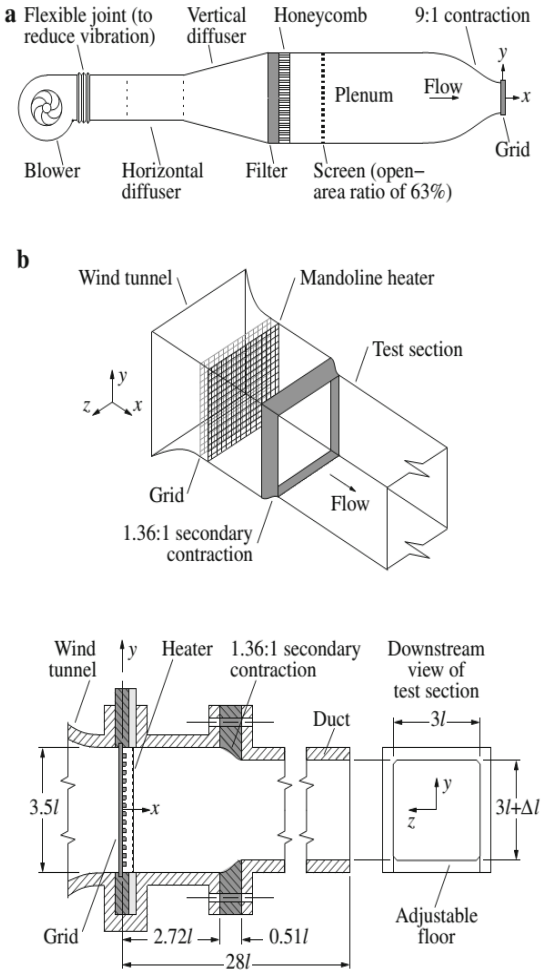

Fig. 2 (a) The wind tunnel (b) The test section with the 1.36:1 secondary contraction downstream of the grid (scale: $l = 0.1m$) (Fig. 2 taken from [9])

A wire screen (with an open area ratio of 63%) and a smooth 9:1 primary contraction in the plenum improve the uniformity of the flow. For the arrangement of the secondary (1.36:1) contraction shown in Fig. 2, the inlet plane of the contraction is at x/M=6.2, 19.2 and 54.2 in case of along the downstream of the three grids. The velocity along the working section to be convected from the grid at say‘s=0 to a downstream position‘s=x’ (e.g. [7]) is given by

$$t = \int_0^x \frac{ds}{\langle U(s) \rangle} \tag{1}$$

where the mean velocity <U(x)> is approximated by the centreline velocity $U_{cl}(x)$ of the wind tunnel flow in the absence of the grid. The angular brackets denote the mean value. The centreline velocity is measured by using a Pitot-static tube and a 100-pa micro-manometer.

For this study, the grid-mesh Reynolds number are $R_M = MU_o/\nu = 1200$, 1474, 4170, 5800, 12900 17950 and 35750 respectively (see Table I). The Taylor microscale Reynolds number $R_\lambda = u'\lambda/\nu$ varies within the range between 6 and 100.

III. Measurements Technique

The velocity fluctuation (u) has been measured simultaneously using a single “hot-wire” probe. The hot wire (diameter $d \approx 2\mu m$ and $d \approx 5\mu m$; length $l = 200d$) is etched from a coil of Wollaston (Platinum). The hot wire measurements are carried and is operated with an ambient constant temperature anemometer (hereafter, CTA) with an over-heat ratio of 1.5. The output signal from CTA circuits passed from the gain units, offset and low pass filtered at a cut –off frequency f_c close to the Kolmogorov frequency f_k ($\equiv U_o/2\pi\eta, \eta = \nu^{3/4}\langle\varepsilon\rangle^{-1/4}$ is the Kolmogorov length scale). Sampling frequency is at least twice or greater than two times of cut-off frequency, (see, Nyquist theory [10]). The hot-wire signals were digitized into a personal computer with a ± 10 V and 16 bit analogue-digital converter.

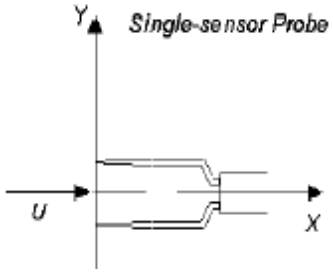

Fig. 3 Geometric configuration of single hot wire probes

IV. Basic Mathematical Presentation of Energy Spectrum

The two –point velocity correlation for homogeneous flow can be defined as

$$R_{ij}(r,t) \equiv \langle u_i(x+r,t)u_j(x,t) \rangle \tag{2}$$

and is independent of x in homogeneous turbulence.

At $x = 0$ it is

$$R_{ij}(0,t) = \langle u_i u_j \rangle = u'^2 \delta_{ij}. \tag{3}$$

In grid turbulence where the turbulent production is zero once turbulence is established, the transport equation of the turbulent kinetic energy $q(t) = (3/2)u'^2(t)$ simplifies to:

$$\frac{dk}{dt} = -\varepsilon \tag{4}$$

where, ε is the dissipation rate. $R_{ij}(r)$ can be expressed in terms of longitudinal $f(r,t)$ and transvers $g(r,t)$ autocorrelation function

$$R_{ij}(r,t) = u'^2\left(g(r,t)\delta_{ij} + [f(r,t) - g(r,t)]\frac{r_i r_j}{r^2}\right). \quad (5)$$

The two point velocity correlation $R_{ij}(r)$ and the velocity spectrum tensor $\Phi_{ij}(\mathbf{k})$ are related through a Fourier-transform in homogeneous turbulence:

$$\Phi_{ij}(\mathbf{k}) = \frac{2}{(2\pi)^3}\int_{-\infty}^{\infty}\int\int R_{ij}(r)e^{-ik.r}dr \quad (6)$$

$$R_{ij}(r) = \int_{-\infty}^{\infty}\int\int \Phi_{ij}(\mathbf{k})e^{ik.r}dk \quad (7)$$

here, $\mathbf{k} = \{k_1, k_2, k_3\}$ is the continuous wave number.

The energy spectrum function is defined as

$$E(k) = \oint \frac{1}{2}\Phi_{ii}(\mathbf{k})\delta(|\mathbf{k}| - k)d\mathbf{k} \quad (8)$$

where, k is an independent variable.

The one dimensional spectra $E_{ij}(k_1)$ are defined to be twice the one dimensional Fourier transform of $R_{ij}(e_1 r_1)$:

$$E_{ij}(k_1) \equiv \frac{1}{\pi}\int_{-\infty}^{\infty} R_{ij}(e_1 r_1)e^{-ik_1 r_1}dr_1 \quad (9)$$

now, assume that $i = j$, so that one dimensional energy spectrum along the longitudinal direction is

$$E_u(k_1) = \frac{2}{\pi}\langle u_1\rangle^2 \int_0^{\infty} f(r_1)\cos(k_1 r_1)dr_1 \quad (10)$$

however, the Kolmogorov velocity spectrum as

$$E_u(k_1) = \varepsilon^{2/3}k_1^{-5/3}\phi(k_1\eta) \quad (11)$$

where, $\phi(k_1\eta)$ is the compensated Kolmogorov spectrum function and it can be write as

$$\phi(k_1\eta) = (k_1\eta)^{5/3}\varphi(k_1\eta) \quad (12)$$

here, $\varphi(k_1\eta)$ is a universal non-dimensional energy spectrum function.

V. Results and Discussion

Fig. 4 shows that the velocity and the 5/3 compensated spectrum at $R_\lambda = 17$. For comparison, the velocity spectrums of [11] $R_\lambda = 60.7$ is reported also on the Fig. 4 (a). It is clear that the 5/3 scaling does not appear in Fig. 4 (a) as illustrated by the lack of a plateau in Fig. 4 (b). This is in effect expected at this low Reynolds number where the existence of the 5/3 region is knows not to exit, i.e. there is no inertial range at low Reynolds number, because the "length" scale separation between the large and small scales is too small.

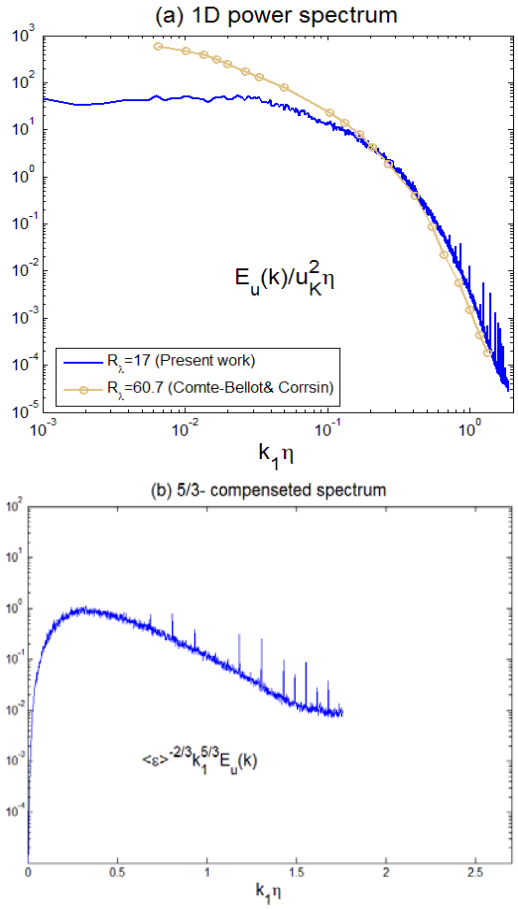

Fig. 4 (a) Kolmogorov non-dimensional 1D velocity spectrum (b) 5/3 compensated spectrum at UotM=200, $R_M = 4170$ and $R_\lambda = 17$

In order to assess the Kolmogorov scaling, a reference Kolmogorov normalized spectrum satisfying the Kolmogorov similarity is required. For example, one can use the spectrum obtained from the analytical expression such as [7] and [8].

In Fig. 5, we present the energy spectrum based on Pope's model (2000) with our present measured spectra at $x/M = 50$ and for three velocities $U_o = 12.75$ m/s, 6.4 m/s and 4.6m/s corresponding to $R_\lambda = 86$, 58 and 46 (the spatial resolution $\eta/l = 0.63, 1.04$ and 1.40 respectively). The measured spectrums are obtained in the Lsq43 perforated grid turbulence.

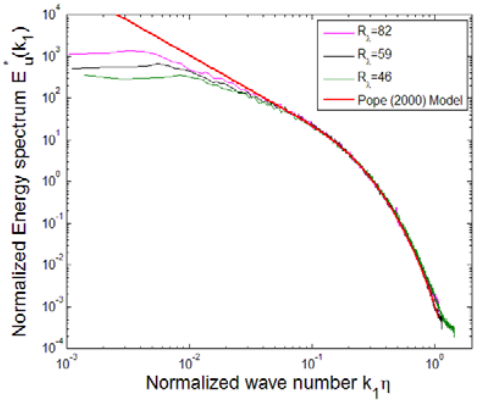

Fig. 5 Measured (Present) and calculated [12] one dimensional longitudinal velocity spectra at x/M=50

The Pope's model is

$$E_u(k_1) = c_1 < \varepsilon >^{2/3} k_1^{-5/3} f_\eta(k_1\eta) \quad (13)$$

$$f_\eta(k_1\eta) = \exp\left\{-c_2\left\{\left[(k_1\eta)^4 + c_3{}^4\right]^{1/4}\right\} - c_3\right\}$$

with constant $c_1 = 7.2, c_2 = 0.5$ and $c_3 = 0.15$ which provides a good matching between the calculated and measured spectra (e.g. [6]). Not though that the measured spectra do not show a 5/3 region, or only over a very small portion. There is however a very good collapse in the dissipative range $(k_1\eta \geq 0.2)$, confirming that the first similarity law holds. However, there is no collapse in the spectra which is shown in Fig. 6, where $R_\lambda = 23$, 17 and 10 (spatial resolution $\eta / l = 0.56$, 1.02 and 0.63 respectively).

The results are consistent with the results of [5] and [6] and confirm the Kolmogorov scaling is breaks down.

In order to determine the critical value of R_λ which the scaling is no longer valid, several spectra are measured in grid turbulence at R_λ ranging from 6 to 65 and reported in Fig. 7.

At $R_\lambda = 25$, the spectra show a departure from the spectrums at relatively higher Reynolds number R_λ, suggesting that the Kolmogorov universality breakdown has occurred. This points to a value of about $30 \geq R_{\lambda,c} \geq 20$, at which the Kolmogorov normalization is no longer valid. It is interesting to note that using a phenomenological analysis [6] showed that a possible critical value of $R_{\lambda,c}$ is about 40.

While one could have expected that the Kolmogorov scaling eventually breaks down when the Reynolds number reaches a critical value, it was not a trivial matter to determine the actual value. One may inquire if this breakdown is linked to the fact that the turbulence may have reached its final stage of decay, or at least approached it. To determine if the turbulence has reached or is close to the final stage of decay, we look at the decay exponent (n) (power law decay: $q'^2 \sim x^{-n}$).

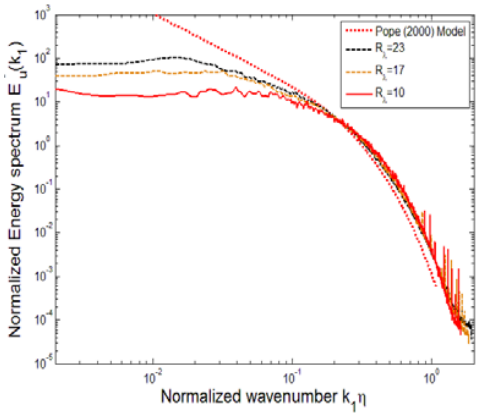

Fig. 6 Measured (solid line and das dotted) and calculated (dotted line) one dimensional longitudinal velocity spectra at different $R_\lambda = 23, 17$ and 10

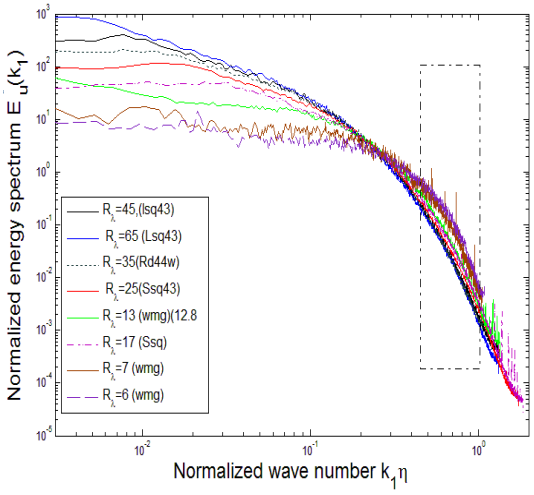

Fig. 7 Deviation of velocity energy spectrum at low Reynolds number R_λ

Table I shows the different conditions for the three grids with the decay exponent rate (n). U_o is the free stream velocity, virtual origin $U_o t_o / M$.

TABLEI
INITIAL CONDITIONS OF THREE DIFFERENT GRIDS AND DECAY EXPONENTS (N)

Grids	Initial Condition	U_o m/s	$U_o t_o / M$	$-n$	R_λ	R_M
Lsq43	1.36:1 Contraction	12.75	6.1	1.13	100-82	35750
		6.4	6.6	1.14	65-58	17900
		4.6	5.6	1.15	50-45	12950
Ssq43	1.36:1 Contraction	6.4	-2.0	1.26	30-23	5800
		4.6	-2.0	1.36	23-17	4170
Wmg36	1.36:1 Contraction	4.6	-28.0	1.50	10-7	1474
		3.6	-28.0	1.52	9-6	1200

Within the final period of decay i.e. $R_\lambda \to 0$, the value of n is -3/2 according to [13] or -5/2 according to [14]. We

reported in Fig. 8, the value of $-n$ as function of R_λ. There is a clear trend of increasing $-n$ with decreasing R_λ. It is however difficult at this stage to extrapolate the results to $R_\lambda = 0$ as more data points need to be taken a lower value of the Reynolds number.

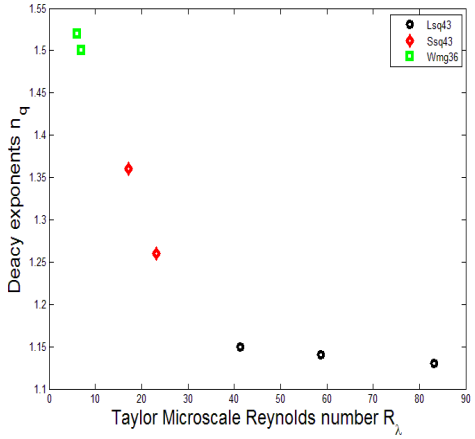

Fig. 8 Decay exponent (n) decreasing function of Taylor microscale Reynolds number R_λ

Nevertheless, the values of R_λ at which $-n$ starts to deviate significantly correspond to those at which the Kolmogorov scaling breakdowns, suggesting that the breakdown may be interconnected to the approach towards the final period of decay.

VI. Conclusion

The present paper reports the measurements of velocity spectra at low Reynolds numbers in grid turbulence with the view to determine whether the Kolmogorov scaling is valid or not. The results clearly indicate that such scaling holds until the Reynolds number R_λ drops to a critical value of about 30-25. Below this value the Kolmogorov normalized spectra deviate from the universal Kolmogorov spectrum. It is speculated that the Kolmogorov scaling breakdowns is related to the fact that turbulence approaches its final stage of decay.

Acknowledgment

The Australian Research council is gratefully acknowledged for the financial support.

References

[1] A.N. Kolmogorov, "The local structure of turbulence in incompressible viscous fluid for very large Reynolds numbers", Dokl.Akad.Nauk SSSR 30. 1941,299 (Proc.R.Soc.London.Ser.A 434, 1991, 9-13).
[2] L. Djenidi, "Lattice –Boltzmann simulation of grid –generated turbulence," J.Fluid Mech., vol. 552, 1964, pp. 13-35.
[3] P.Burattini,P.Lavoie, A.Agrawal, L.Djenidi and R.A. Antonia, "Power lawod decaying homogeneous isotropic turbulence at low Reynolds number", Phy.Rev.E73 (066304), 2006, 1-7.
[4] L.Djenidi and R.A. Antonia, "A spectral chart method for estimating the mean turbulent kinetic energy dissipation rate,"*Exp.Fluids,*vol 53, 2012, pp. 1005-1013.
[5] N.N. Mansour and A.A. Wray, "Decay of isotropic turbulence at low Reynolds number," *Phys. Fluids,* vol. 6, no 2, 1994, pp. 808-814.
[6] L.Djenidi, R.A. Antonia and S.Tardu,"Breakdown of Kolmogorov's scaling in grid turbulence," in *Proc.1 4th European Turbulence Conference,*, France, 2013.
[7] G. Comte-Bellot and S. Corrsin, "The use of a contraction to improve the isotropy of grid turbulence," *J. Fluid Mech.*vol.25, part 4, 1966, pp. 657-682.
[8] Y.H. Pao, "Structure of turbulent velocity and scalar fields at large wavenumbers,"Phys.Fluids, vol. 8, no.6, 1965, pp. 1063-1075.
[9] S.K.Lee, A. Benaissa, L. Djenidi, P.Lavoie and R.A.Antonia ," Decay of passive-scalar fluctuations in slightly stretched grid turbulence", Exp Fluids,2012,
[10] W.D. Stanley, "Digital signal processing," Reston publishing company, inc, Reston, Virginia, 1975, pp.48-49.
[11] G. Comte-Bellot and S. Corrsin, ", Simple Eulerian time correlation of full and narrowband velocity signals in grid generated,` isotropic turbulence" J.Fluid Mech., Vol. 48, 1971, pp. 273-337.
[12] S.B. Pope, "Turbulent flows," Cambridge Press, UK.
[13] G. K. Batchelorand A. A. Townsend, "Decay of turbulence in the final period," Proc. R. Soc. London Ser. A 194, 1948, pp.
[14] P.G. Saffman, "The large- scale structure of homogeneous turbulence," J. Fluid Mech. 27, 581, 1967.